Comparison of the Diagnostic Accuracy of Contrast-Enhanced MRI and Diffusion-Weighted MRI in the Differentiation Between Uterine Leiomyosarcoma / Smooth Muscle Tumor With Uncertain Malignant Potential and Benign Leiomyoma

Gigin Lin, MD, PhD,[1] Lan-Yan Yang, PhD,[2] Yu-Ting Huang, MD,[1] Koon-Kwan Ng, MD,[1] Shu-Hang Ng, MD,[1] Shir-Hwa Ueng, MD,[3] Angel Chao, MD, PhD,[4] Tzu-Chen Yen, MD, PhD,[5] Ting-Chang Chang, MD,[4]* and Chyong-Huey Lai, MD[4]

Purpose: To compare the diagnostic accuracy of contrast-enhanced (CE) magnetic resonance imaging (MRI) and diffusion-weighted MRI (DWI) in the differentiation between uterine leiomyosarcoma (LMS) / smooth muscle tumor with uncertain malignant potential (STUMP) and benign leiomyoma.

Materials and Methods: A consecutive cohort of 8 LMS/STUMP and 25 benign leiomyomas underwent pelvic MRI exam at 3T. Two radiologists independently evaluated images based on CE-MRI (central nonenhancement at equilibrial phase) and DWI (hyperintensity on b = 1000 s/mm^2 and hypointensity on apparent diffusion coefficients [ADC] map). The ADC values were calculated from b = 0 and 1000 s/mm^2.

Results: CE-MRI yielded a significantly superior diagnostic accuracy (0.94 vs. 0.52) and a significantly higher specificity (0.96 vs. 0.36) than DWI ($P < 0.05$ for both), and remained a comparably high sensitivity as DWI (0.88 vs. 1.00). A combination of DWI and ADC value $<1.08 \times 10^{-3}$ mm^2/s (determined by receiver operating characteristic analysis) improved diagnostic accuracy, sensitivity, and specificity of DWI to 0.88, 0.88, and 0.88, respectively, by post-hoc analysis based on the same study cohort.

Conclusion: For prospective differentiation between uterine LMS/STUMP and benign leiomyoma, CE-MRI can provide accurate information and is preferable to DWI. Combination of DWI and ADC values can achieve a comparable diagnostic accuracy to CE-MRI.

J. MAGN. RESON. IMAGING 2016;43:333–342.

View this article online at wileyonlinelibrary.com. DOI: 10.1002/jmri.24998

Received Apr 27, 2015, Accepted for publication Jun 23, 2015.

*Address reprint requests to: T.-C.C., Department of Obstetrics and Gynecology, Gynecology Oncology Research Center, Chang Gung Memorial Hospital and Chang Gung University, Linkou Medical Center, 5 Fuhsing Street, Guishan, Taoyuan 333, Taiwan. E-mail: tinchang.chang@gmail.com

From the [1]Department of Medical Imaging and Intervention, Chang Gung Memorial Hospital and Institute for Radiological Research, Chang Gung University, Linkou Medical Center, Guishan, Taoyuan, Taiwan; [2]Clinical Trial Center, Chang Gung Memorial Hospital and Chang Gung University, Linkou Medical Center, Guishan, Taoyuan, Taiwan; [3]Department of Pathology, Chang Gung Memorial Hospital and Chang Gung University, Linkou Medical Center, Guishan, Taoyuan, Taiwan; [4]Department of Obstetrics and Gynecology, Gynecology Oncology Research Center, Chang Gung Memorial Hospital and Chang Gung University, Linkou Medical Center, Guishan, Taoyuan, Taiwan; and [5]Department of Nuclear Medicine and Center for Advanced Molecular Imaging and Translation, Chang Gung Memorial Hospital and Chang Gung University, Linkou Medical Center, Guishan, Taoyuan, Taiwan

Leiomyosarcoma (LMS) is a rare malignant tumor with an extremely poor prognosis, with 5-year overall survival rates between 19% and 65%.[1,2] In contrast, leiomyomas are common benign tumors of uterus, affecting nearly 80% of women during their lifetime.[3] Another rare entity, uterine smooth muscle tumor with uncertain malignant potential (STUMP), is also clinically considered of low malignant potential.[4] LMS/STUMP and benign leiomyomas share a similar clinical presentation as rapidly growing uterine tumors, leading to ~0.5% of resected tumors with preoperative diagnosis of leiomyoma are unexpectedly revealed to be LMS based on final histopathology.[5] Preoperative diagnosis of uterine LMS/STUMP is increasingly important due to emerging nonhysterectomy options for symptomatic leiomyoma, for instance, laparoscopic myomectomy,[6] uterine artery embolization,[7] or high-intensity focused ultrasound.[8] Because the myometrial location of tumors renders tissue diagnosis from endometrial samplings extremely difficult, preoperative imaging diagnosis plays a crucial role.[9]

MRI is widely accepted as the standard for preoperative evaluation for clinical suspicion of LMS/STUMP, commonly presenting as large uterine masses with hemorrhage and necrosis,[10] with high signal on T_1-weighted images (T_1WI) and T_2-weighted images (T_2WI) and the presence of unenhanced pocket-like areas on contrast-enhanced (CE)-MRI.[11] However, clearly distinguishing between LMS/STUMP and benign leiomyomas by MRI remains challenging due to not infrequently atypical imaging features,[12–14] Recently, diffusion-weighted MRI (DWI) showed promise in differentiating between LMS and leiomyomas,[15–17] making intravenous gadolinium contrast medium potentially unnecessary for evaluating patients with clinical suspicious of uterine LMS/STUMP.

The purpose of this study was to compare the diagnostic accuracy of CE-MRI and DWI for preoperative differentiation between uterine LMS/STUMP and benign leiomyoma.

Materials and Methods

Study Population

Our Institutional Review Board approved the protocol of this prospective study and informed consent was obtained. The flow diagram of study design is summarized in Fig. 1. We prospectively conducted gynecological MRI examinations for a consecutive series of patients with rapidly growing uterine tumors and suspected to be LMS/STUMP by Gynecology Oncology specialists. The inclusion criteria of clinically suspected uterine sarcoma was based on the following features measured on transvaginal and/or transabdominal ultrasonography: 1) doubling of the perpendicular diameters within 3–6 months, tumor diameter more than 10 cm without symptom presentation, or tumor diameter more than 5 cm with symptom presentation in both pre- and postmenopausal women; 2) tumor diameter more than 5 cm in postmenopausal women.

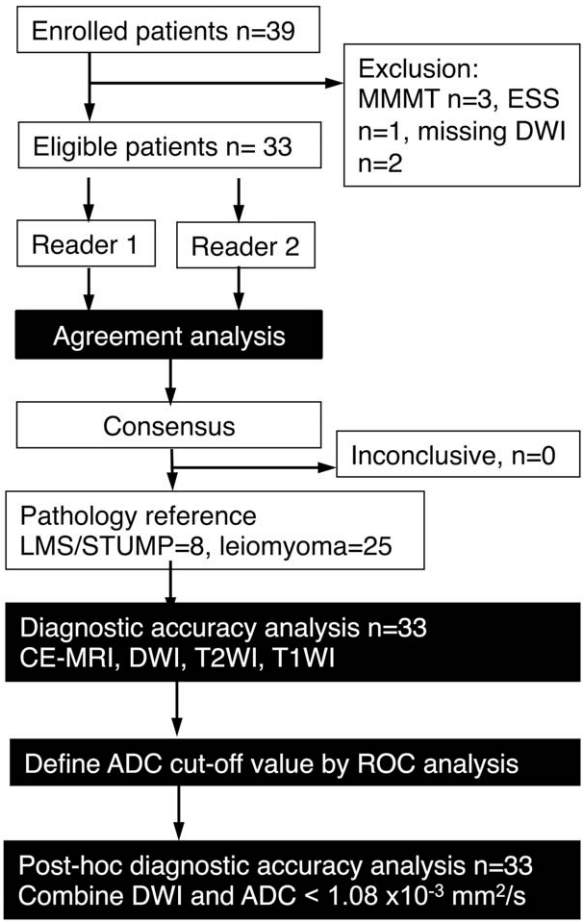

FIGURE 1: Flow diagram of the study design. ADC = apparent diffusion coefficient; CE-MRI = contrast enhanced magnetic resonance imaging; DWI = diffusion-weighted imaging (b = 1000 s/mm^2); ESS = endometrial stromal sarcoma; LMS = leiomyosarcoma; MMMT = malignant mixed mesodermal tumor; ROC = receiver operating characteristic; STUMP = smooth muscle tumor with uncertain malignant potential; T_1WI = T_1-weighted imaging; T_2WI = T_2-weighted imaging.

The exclusion criteria were: i) endometrial biopsy proven to be malignancy other than LMS/STUMP, eg, endometrial cancer, carcinosarcoma, endometrial stromal sarcoma, adenosarcoma; ii) the presence of any MRI contraindication (cardiac pacemaker or defibrillator, insulin pump, aneurysm clip, implanted neural stimulator, cochlear implant, metal shrapnel or bullet, etc.); iii) the presence of pelvis or hip metal prostheses; iv) contraindication of intravenous gadolinium contrast medium (allergy history or estimated glomerular filtration rate [eGFR] lower than 30 mL/min/m^2 and/or are undergoing chronic dialysis treatment); v) inability to give informed consent; and vi) any contraindication for surgery.

MRI Protocol

MR images were acquired using a 3.0T system (Trio Tim, Siemens Medical Systems, Erlangen, Germany) using phased-array body coils to cover the entire pelvis, with previously reported parameters.[18] The acquisition protocol is summarized in Table 1. In brief, we applied T_1WI and T_2WI turbo spin-echo sequences to scan the pelvis. DWI exam was carried out using a single-shot echo-planar technique with fat-suppression. The diffusion-weighted gradients

TABLE 1. Acquisition Protocol

	CE-MRI	DWI	T2WI	T1WI
Pulse sequence	Turbo spin echo	Single-shot echo-planar	Turbo spin echo	Turbo spin echo
Orientation	Axial and sagittal	Axial and sagittal	Axial and sagittal	Axial
Slice thickness/Gap (mm)	4/1	4/1	4/1	4/1
Repetition time (msec)	567	3300	5630	626
Echo time (msec)	10	79	87	11
Field of view (cm)	20	30	20	20
Acquisition matrix (phase x frequency)	256 × 320	128 × 128	256 × 320	256 × 320
Averages (NEX)	2	4 (both b-0 and b-1000)	3	2
Echo train length (ETL)	5	120	13	3
Flip angle	150	180	150	150
GRAPPA factor	2	2	2	2
Fat saturation	CHESS	CHESS	None	None
Acquisition time (sec)	185	63	176	133

CE-MRI = contrast enhanced magnetic resonance imaging; ; CHESS = chemically selective suppression; DWI = diffusion-weighted imaging (b = 1000 s/mm^2); GRAPPA = generalized auto-calibrating partially parallel acquisition; T1WI = T1-weighted imaging. T2WI = T2-weighted imaging.

were applied orthogonally in slice-selective, phase encoding, and readout directions. Apparent diffusion coefficient (ADC) maps were generated from isotropic DWI with b values of 0 and 1000 s/mm^2, by calculating the slope of the logarithmic decay curve for SI against b value (Syngo, Siemens). At about 120–180 seconds equilibrial phases after intravenous injection of 0.1 mmol/kg body weight of contrast medium (Gadopentetate Dimeglumine, Magnevist, Schering, Berlin, Germany) followed by a 20-mL saline flush at a rate of 2–3 mL/sec, contrast-enhanced T_1WI was acquired. The study was performed during normal respiration. No premedication or antiperistalsis agent was utilized.

MRI Analysis

Two radiologists with 29 (K.K.N.) and 7 years experience (Y.T.H.) in gynecologic radiology interpreted images, without prior knowledge of clinical and histological information. The imaging review process was carried out independently with a dedicated image processing software (OsiriX v5.6, Los Angeles, CA) on an offline Mac OS workstation (MacBook Pro, Apple, Cupertino, CA). Images were interpreted by K.K.N. and Y.T.H. separately, and consensus was made on joint reading sessions weekly. When there were multiple tumors within the same uterus, the largest tumor was evaluated, and its tumor size was measured.[14–16] Imaging parameters including CE-MRI, DWI, T_2WI, and T_1WI were assessed without cross-reference to one another. CE-MRI positivity was based on identification central nonenhancement (CNE), well-demarcated pocket-like nonenhanced areas on postcontrast T_1WI,[11] which was evaluated using a visual qualitative assessment of pre- and postcontrast images without region of interest (ROI). The largest single diameter of the nonenhancing part of the tumor was divided by the largest single diameter of tumor measured on contrast-enhanced images to generate the necrosis-to-tumor ratio. Multiple small well-defined nonenhanced areas scattering in the periphery or throughout the tumor based on visual assessment were not regarded as CNE. DWI positivity was deemed as more than 50% signal higher than that of the outer myometrium on high b-value DWI (b = 1000 s/mm^2) and a lower signal on ADC maps. The ADC values of each primary tumor were measured by manually drawn ROIs on the console within main tumors on the largest tumor plane on T_2WI axial images, encompassing all the tumor that was nonnecrotic as judged from the T_1WIs and T_2WIs, with the ROIs copied from T_2WIs onto the ADC map, excluding the necrotic/nonenhancing portion. The ADC values measured by the two readers independently were averaged to be the representative ADC value for each tumor. T_1WI positivity was defined as the presence of any mass area with higher signal than fatty bone marrow of the pubis symphysis.[11] T_2WI positivity was defined as more than half of the mass with signal higher than that of the outer myometrium on T_2WIs.[11,14]

Histopathologic Analysis

The reference standard used in this study was surgical histopathology, reviewed by a pathologist (S.H.U.) who specialized in gynecologic pathology for 11 years. The histopathologic diagnosis was performed based on criteria advocated by Bell et al,[19] ie, the presence of coagulative necrosis, cellular atypia, cellularity, and the number of mitotic figures in 10 high-power fields, as evaluated on hematoxylin-eosin (H&E)-stained slides. The largest uterine tumor was analyzed in the presence of multiple tumors in the same patient.

TABLE 2. Demographics of the Study Participants

	LMS/STUMP		Benign leiomyoma	
Total number, n (%)	8 (24%)		25 (76%)	
Age (year)				
Median (range)	47 (40 –55)		47 (32–53)	
Menopausal status				
Premenopausal	7		21	
Postmenopausal	1		4	
Tumor size (cm)				
Median (range)	12.8 (5.5–20.0)		9.7 (4.5–16.7)	
Pathology, *n*	LMS	6	Cellular leiomyoma	3
	STUMP	2	Infarcted leiomyoma	3
			Degenerated leiomyoma	8
			Ordinary leiomyoma	11
Pathology staging, *n*	T1bN0M0	5		
	T2aN0M0	2		
	T2bN0M0	1		
Primary surgery, *n* (%)	ATH + BSO	8	ATH	24
			Hysteroscopic hysterectomy	1

ATH = abdominal total hysterectomy; BSO = bilateral salpingo-oophorectomy; LMS = leiomyosarcoma; STUMP = smooth muscle tumor with uncertain malignant potential.

Statistical Analysis

Data were analyzed with MedCalc for Windows, v. 12.6.1.0 (MedCalc Software, Mariakerke, Belgium). Mann–Whitney *U* analysis was used to compare age, tumor size, and ADC values between patients with LMS/STUMP or benign leiomyoma. Reader agreement regarding the imaging parameters was analyzed with weighted kappa statistics, with $\kappa < 0.40$ indicating poor agreement, $0.40 \leq \kappa \leq 0.75$, fair to good agreement, and $\kappa > 0.75$, excellent agreement.[20] The diagnostic accuracy, sensitivity, specificity, positive predictive value (PPV), and negative predictive value (NPV) for each imaging datasets (CE-MRI, DWI, T_2WI, T_1WI, respectively) was calculated independently with related exact 95% confidence intervals (CIs). The McNemar's test was used to compare the sensitivity, specificity, and diagnostic accuracy between CE-MRI and non-MRI parameters (DWI, T_2WI, or T_1WI). Receiver operating characteristic (ROC) analysis was used to identify the cutoff ADC value. Areas under the ROC curve (AUC) were applied to compare the diagnostic performance of CE-MRI versus DWI, T_2WI, T_1WI, and a combination of DWI and ADC values. A value of $P < 0.05$ (two-sided) was considered statistically significant.

Results

Patients

In total, 33 patients were eligible for final analysis, with final histopathologic diagnosis as LMS ($n = 6$), STUMP ($n = 2$) or benign leiomyoma ($n = 25$). None of the eligible patients had a history of previous pelvic irradiation. The demographics of eligible patients are summarized in Table 2. The time interval of MR examination and operation ranged from 3–65 days (median, 14 days). No remarkable adverse event was recorded during the MRI studies. There was no significant difference between the LMS/STUMP group and benign leiomyoma group regarding age ($P = 0.74$, Mann–Whitney *U* test) or tumor size ($P = 0.12$).

Reader Agreement and Diagnostic accuracy

Reader agreements were excellent for the CE-MRI ($\kappa = 0.921$), DWI ($\kappa = 0.847$), T_2WI ($\kappa = 0.836$), and T_1WI ($\kappa = 0.873$). The consensus MRI characteristics for the study participants are summarized in Table 3. CE-MRI was found to be the most characteristic imaging feature of LMS/STUMP, and yielded a significantly higher diagnostic accuracy of 0.94, as compared with that of DWI, T_2WI, or T_1WI criteria (0.52, 0.46, 0.67, respectively, $P < 0.05$ for all), as summarized in Table 4. The sensitivities of CE-MRI, DWI or T_2WI were 0.88, 1.00, 0.88, respectively, all significantly higher than that of T_1WI criteria (0.63, $P < 0.05$ for all). The specificity of CE-MRI was 0.96, significantly

TABLE 3. MRI Characteristics for the Study Participants

No.	Pathological diagnosis	CE-MRI	DWI	T2WI	T1WI	ADC
1	Leiomyosarcoma	+	+	+	+	0.75
2	Leiomyosarcoma	+	+	+	+	0.86
3	Leiomyosarcoma	+	+	+	+	0.83
4	Leiomyosarcoma	+	+	+	+	0.93
5	Leiomyosarcoma	+	+	+	−	1.08
6	Leiomyosarcoma	+	+	+	−	1.85
7	STUMP	+	+	+	+	1.01
8	STUMP	−	+	−	−	0.82
9	Cellular leiomyoma	−	+	+	+	1.35
10	Cellular leiomyoma	−	+	+	−	0.89
11	Cellular leiomyoma	−	+	+	−	2.04
12	Infarcted leiomyoma	+	+	+	+	1.68
13	Infarcted leiomyoma	−	+	+	+	1.30
14	Infarcted leiomyoma	−	−	−	−	0.70
15	Degenerated leiomyoma	−	+	+	+	1.37
16	Degenerated leiomyoma	−	+	+	+	1.06
17	Degenerated leiomyoma	−	+	+	−	1.10
18	Degenerated leiomyoma	−	+	−	+	1.26
19	Degenerated leiomyoma	−	−	+	−	1.43
20	Degenerated leiomyoma	−	−	−	+	1.05
21	Degenerated leiomyoma	−	−	−	−	1.19
22	Degenerated leiomyoma	−	−	−	−	0.94
23	Ordinary leiomyoma	−	+	+	+	1.23
24	Ordinary leiomyoma	−	+	+	−	1.21
25	Ordinary leiomyoma	−	+	+	−	1.25
26	Ordinary leiomyoma	−	+	+	−	1.30
27	Ordinary leiomyoma	−	+	+	−	1.14
28	Ordinary leiomyoma	−	+	+	−	1.16
29	Ordinary leiomyoma	−	+	−	−	0.72
30	Ordinary leiomyoma	−	−	+	−	1.07
31	Ordinary leiomyoma	−	−	+	−	1.23
32	Ordinary leiomyoma	−	−	−	−	1.14
33	Ordinary leiomyoma	−	−	−	−	1.13

ADC = apparent diffusion coefficient value (10^{-3} mm^2/sec); CE-MRI = contrast enhancement magnetic resonance imaging; DWI = diffusion-weighted imaging; STUMP = smooth muscle tumors with uncertain malignant potential; T1WI = T1-weighted images; T2WI = T2-weighted images.

higher than that of DWI, T_2WI, or T_1WI criteria (0.36, 0.32, 0.68, respectively, $P < 0.05$ for all). Based on ROC analysis, the AUC of CE-MRI in diagnosis of LMS/STUMP was 0.92, which was significantly superior to that of DWI (AUC = 0.68, $P < 0.01$), T_2WI (AUC = 0.60, $P < 0.0001$) or T_1WI (AUC = 0.65, $P < 0.005$) (Fig. 2).

TABLE 4. Diagnostic Accuracy in Detection of Uterine LMS/STUMP Based on Magnetic Resonance Imaging Parameters

	n	TP	TN	FP	FN	Accuracy	Sensitivity	Specificity	PPV	NPV
CE-MRI	33	7	24	1	1	0.94 (0.80–0.99)	0.88 (0.47–1.00)	0.96 (0.80–1.00)	0.88 (0.47–1.00)	0.96 (0.80–1.00)
DWI	33	8	9	16	0	0.52 (0.34–0.69)*	1.00 (0.63–1.00)	0.36 (0.18–0.58)*	0.33 (0.16–0.55)	1.00 (0.66–1.00)
T2WI	33	7	8	17	1	0.46 (0.28–0.64)*	0.88 (0.47–1.00)	0.32 (0.15–0.54)*	0.29 (0.13–0.51)	0.89 (0.52–1.00)
T1WI	33	5	17	8	3	0.67 (0.48–0.82)*	0.63 (0.25–0.92)*	0.68 (0.47–0.85)*	0.39 (0.14–0.68)	0.85 (0.62–0.97)

Data are means and numbers in parentheses are 95% confidence intervals.
CE-MRI = contrast enhanced magnetic resonance imaging; DWI = diffusion-weighted imaging (b = 1000 s/mm^2); FP = false positive; FN = false negative; NPV = negative predictive value; PPV = positive predictive value; T1WI = T1-weighted imaging. T2WI = T2-weighted imaging; TP = true positive. TN = true negative. *$P < 0.05$, McNemar's comparing accuracy, sensitivity and specificity with CE-MRI.

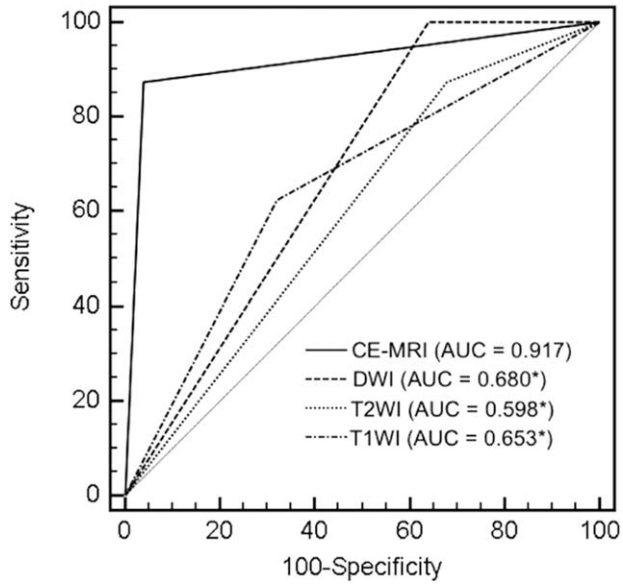

FIGURE 2: Receiver operating characteristic (ROC) analysis of the area under the ROC curve (AUC) of the following criteria: central nonenhancing area (CNE), hyperintensity on diffusion-weighted imaging (DWI), hyperintensity on T_1-weighted images (T_1WI), and hyperintensity on T_2-weighted images (T_2WI). *$P < 0.05$.

ADC Values of Tumors and Post-hoc Accuracy Analysis

The ADC value ($\times 10^{-3}$ mm^2/s) of LMS/STUMP (median 0.89, range 0.74–1.85) was significantly lower than that of benign leiomyomas (median 1.19, range 0.70–2.04, $P < 0.05$, Mann–Whitney U test). However, overlap of ADC values were noted among LMS (mean ± standard deviation, 1.05 ± 0.41), STUMP (0.92 ± 0.13) and benign leiomyomas such as cellular (1.43 ± 0.58), infarcted (1.23 ± 0.50), degenerated (1.17 ± 0.17), or ordinary leiomyomas (1.14 ± 0.16), as shown in Fig. 3. The combination of DWI and ADC cutoff value of 1.08 $\times$ 10^{-3} mm^2/s (determined by ROC analysis) yielded a diagnostic performance comparably high as CE-MRI, with an accuracy, sensitivity, and specificity of 0.88, 0.88, and 0.88, respectively, based on the post-hoc analysis of the same cohort. The AUC of combination of DWI and ADC in diagnosis of LMS/STUMP was 0.74, which showed no significant difference between that of CE-MRI ($P = 0.14$).

Central Nonenhancement (CNE) and Histopathological Correlation

CNEs were appreciated in all of the six LMSs and one of the two STUMPs, showing a concave interface outlined by peripheral component, with a median necrosis-to-tumor ratio of 74% (range 53–89%). CNE corresponded to area of coagulative necrosis, ie, abrupt transition from viable cells to ghost cells (Fig. 4). Notably, the only false negative of CE-MRI was a STUMP without coagulative necrosis on final pathology. On the contrary, 19 benign leiomyomas

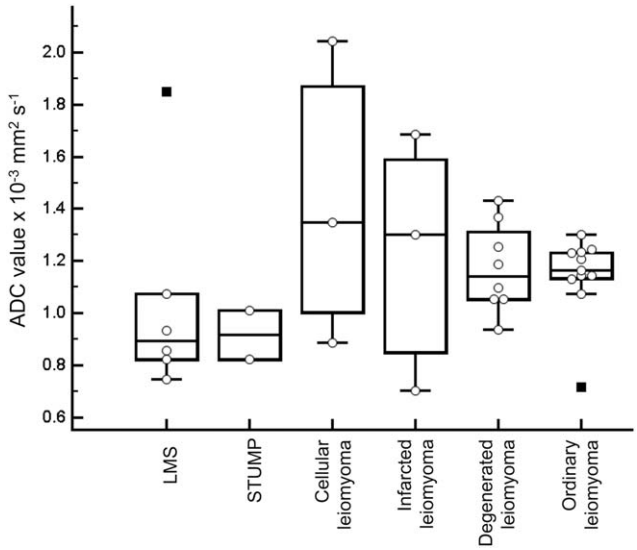

FIGURE 3: ADC values of tumors. The ADC value of LMS/STUMP was significantly lower than that of benign leiomyomas but with a remarkable overlap. LMS = leiomyosarcoma; STUMP = smooth muscle tumor with uncertain malignant potential.

showed homogenous enhancement, with the other six cases (24%) exhibiting scattered, small nonenhancing areas, corresponding to bands of hyalinized collagen of varying thickness between the viable cells and the necrotic foci microscopically (Fig. 5). The only false positive of CE-MRI was a benign infarcted leiomyoma on final pathology.

Discussion

Our results demonstrated that CE-MRI yielded significantly higher diagnostic accuracy and specificity as compared with DWI, in differentiation between LMS/STUMP and benign leiomyoma. The excellent agreement between junior and senior readers supported CE-MRI as an objective method for preoperative MRI evaluation. Our study results are supported by Tanaka et al,[11] showing an overall accuracy of 0.87, a sensitivity of 0.73, and a specificity of 1.00 of using CE-MRI for diagnosis of LMS/STUMP.[11] CE-MRI also demonstrated a diagnostic accuracy superior to T_1WI or T_2WI. Detection of scattered foci of hemorrhage in LMS/STUMP was seen as areas of hyperintensity on T_1WI.[11,21] Intratumoral T_2 hyperintensity, however, is not a reliable indicator for malignancy, because T_2 hyperintensity has been reported in benign leiomyoma especially with degeneration.[12,22] In such cases, CE-MRI was proven superior to T_2WI especially in detecting tumor necrosis[13] and improvement of PPV.[23]

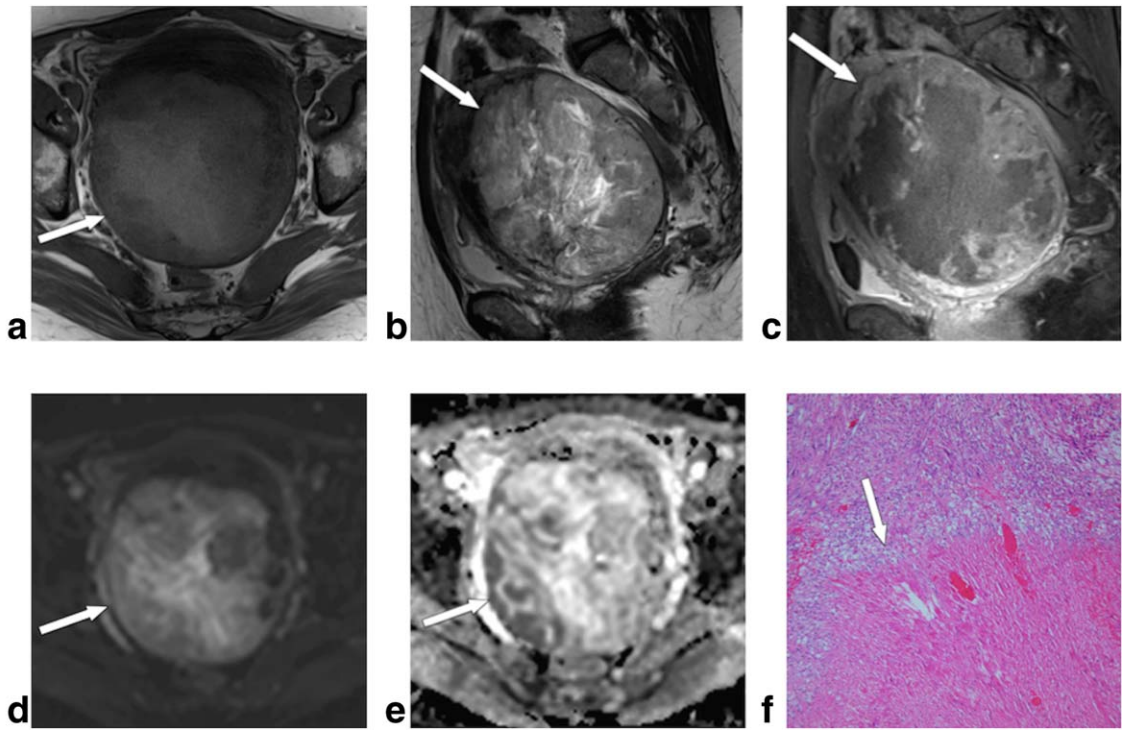

FIGURE 4: A47-year-old woman with histologically proved leiomyosarcoma. a: T_1-weighted image shows tumor as well-defined mass lesion with high signal intensity confined within myometrium (arrow). b: T_2-weighted image shows tumor as bulky mass lesion with heterogeneously high signal intensity (arrow) compared with adjacent normal outer myometrium. c: Contrast-enhanced T_1-weighted image shows tumor containing concave interface outlined by peripheral enhancing soft tissue component. Well-demarcated unenhanced areas involving more than 79% of tumor mainly in the inner or deep portions (arrow). d: Diffusion-weighted image shows tumor as area of mildly and heterogeneous hyperintensity (arrow) in contrast to dark background. e: Tumor ADC value of 0.83 × 10^{-3} mm^2/s. f: Histopathologic examination demonstrates coagulative necrosis (arrow), an abrupt transition from viable cells to ghost cells without an interposed zone of granulation tissue or hyalinized tissue between viable and necrotic cells, characteristics of leiomyosarcoma (arrow, hematoxylin and eosin stain 100×).

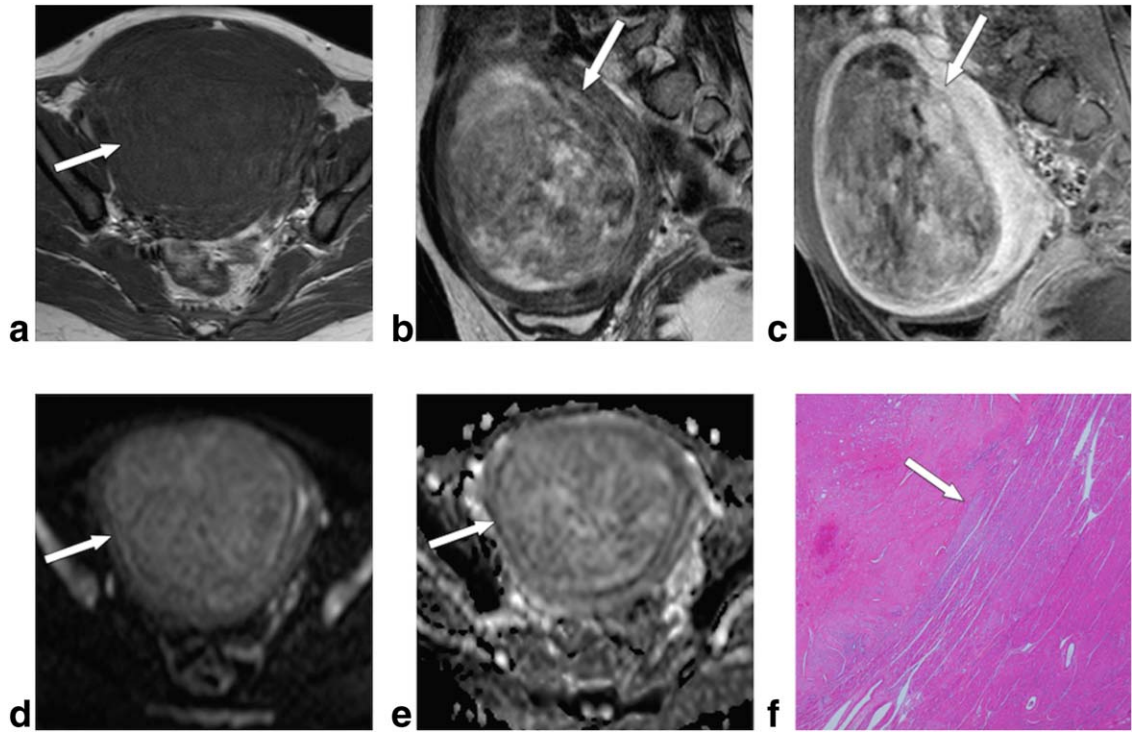

FIGURE 5: A 45-year-old woman with histologically proved benign leiomyoma. a: T_1-weighted image shows tumor as well-defined mass lesion with low signal intensity confined within myometrium (arrow). b: T_2-weighted image shows tumor as bulky mass lesion with heterogeneously high signal intensity (arrow) compared with adjacent normal outer myometrium. c: Contrast-enhanced T_1-weighted image shows tumor as a heterogeneously enhanced lesion containing multiple small well-defined nonenhanced areas scattering at the periphery or throughout the tumor (arrow). d: Diffusion-weighted image shows tumor as area of mild hyperintensity (arrow) in contrast to dark background. e: ADC value of 1.10×10^{-3} mm^2/s. f: Histopathologic examination demonstrates hyaline necrosis, with bands of hyalinized collagen of varying thickness between the viable cells and the necrotic foci (arrow, hematoxylin and eosin stain 100×).

Our study showed that hyperintensity on DWI yielded a high sensitivity but a limited specificity, and did not improve the diagnostic accuracy of noncontrast MRI in differentiation between LMS/STUMP and benign leiomyoma. Only with an additional ADC cutoff value of 1.08×10^{-3} mm^2/s did the diagnostic performance of a combination of DWI and ADC values achieve a level as high as CE-MRI, in line with the literature reported diagnostic accuracy of 0.92, sensitivity of 1.00, and specificity of 0.94–1.00, summarized in Table 5.[15–17,24] Although ADC values were consistently lower in LMS/STUMP than benign leiomyoma on both 1.5T[15,17,24] and 3T unit,[18] DWI low-intensity leiomyomas have been reported to have broad ADC values and substantial overlaps,[17] hence all reported ADC value-based accuracies were based by additional post-hoc analysis. Our study exemplified the difficulty of using DWI to differentiate LMS/STUMP and leiomyoma during a prospective data collection, where CE-MRI is preferable to DWI in this regard, because a priori knowledge of ADC cutoff values is not required.

CNE was reported in this study as a characteristic for LMS/STUMP on CE-MRI, which was correlated with areas of coagulative necrosis, a characteristic feature of LMS on histopathology. Indeed, this feature was demonstrated in the figures of previously reported series,[11,23] a review article,[25] and pictorial assays.[10,26,27] Due to an abrupt transitional zone from viable cells to the ghost cells lacking an interposed zone of granulation or hyalinized tissue to support the tumor architecture, areas of coagulative necrosis might be easily deviated by adjacent viable cells, to create a CNE on CE-MRI.[19] In contrast, leiomyomas with hyaline degeneration contain numerous bands of hyalinized collagen interlacing the viable cells and the necrotic focus to support the structure,[19] and exhibit scattered nonenhancing areas throughout the entire tumor on CE-MRI. Of note, the false positivity of CE-MRI—infarcted leiomyoma has also been demonstrated by Cornfield et al,[14] and merits more caution when interpreting the CE-MRI study.

Several limitations of our study should be addressed. First, the small sample size in this study is attributed to the low incidence of LMS/STUMP. For the interest of comparing patients in similar clinical scenarios, our study included only LMS, STUMP, and benign leiomyomas, and prospectively excluded other uterine malignancies such as endometrial cancer, carcinosarcoma, or endometrial stromal sarcoma because their preoperative diagnosis could be made by endometrial biopsy. Therefore, subgroup analyses were not conducted because they are prone to producing misleading results when the sample size is small, and future study with larger scales conducted under a multicenter study

consortium might solve this limitation. Second, although an imaging review process was carried out independently, each radiologist unavoidably evaluated CE-MRI, DWI, T_2WI, and T_1WI parameters at the same reading session in the clinical setting of this prospective study, even though the interpretation criteria had been clearly defined to minimize this bias. Third, this study strictly selected patients (eGFR more than 30 mL/min/m^2 without history of chronic dialysis), in order to minimize the risk of nephrogenic systemic fibrosis in CE-MRI.[28] For patients with impaired renal function unsuitable for intravenous contrast administration, combined DWI and ADC values might offer viable alterations to patients with clinical suspicion of LMS/STUMP. Finally, this is a prospective study looking at a subpopulation of patients who had at baseline high suspicion for uterine malignancy, and the sensitivities and specificities would be different from a general population screening.

In conclusion, for prospective differentiation between uterine LMS/STUMP and benign leiomyoma, CE-MRI can provide accurate information and is preferable to DWI. The combination of DWI and ADC value can achieve a comparable diagnostic accuracy to CE-MRI.

TABLE 5. Summary of Literature ADC Values of LMS/ STUMP and Other Uterine Sarcomas

Authors	Uterine sarcomas ADC value ($\times 10^{-3}$ mm^2/s)	Cellular leiomyoma	Degenerated leiomyoma	Ordinary leiomyoma ADC value ($\times 10^{-3}$ mm^2/s)	ADC cutoff	Histopathology (*n*)	b value	MRI system	Reference
Tamai et al.	1.17 ± 0.15	1.19 ± 0.18	1.70 ± 0.11	0.88 ± 0.27	N/A	LMS (5) and ESS (2)	0, 500	1.5T	15
Namimoto et al.	0.86 ± 0.11	N/A	N/A	1.18 ± 0.24	1.05	LMS (4), ESS (2) and MMMT (2)	0, 1000	3T	16
Sato et al.	0.79 ± 0.21	1.13 ± 0.25	N/A	1.25 ± 0.42	1.10	LMS (5)	0, 1000	1.5T	17
Thomassin-Haggara et al.	0.97 ± 0.26	N/A	N/A	1.40 ± 0.31	1.23	LMS (3), STUMP (5), intravenous leiomyomatosis (1), rhabdomyosarcoma (1), ESS (2), undifferentiated endometrial sarcoma (9) and MMMT(4)	0, 1000	1.5T	24
Lin et al.	1.02 ± 0.35	1.43 ± 0.58	1.17 ± 0.17	1.14 ± 0.16	1.08	LMS (6), STUMP (2),	0, 1000	3T	Current study

ADC = apparent diffusion coefficient; ESS = endometrial stromal sarcoma; LMS = leiomyosarcoma; MMMT = malignant mixed mesodermal tumor; STUMP = smooth muscle tumor with uncertain malignant potential.

Acknowledgments

Contract grant sponsor: Chang Gung Medical Foundation; Contract grant numbers: CMRPG-370444 and 290262; Contract grant sponsor: National Science Council, Taiwan; Contract grant numbers: NSC100-2325-B-182-008, NSC 103-2314-B-182A-006 and NMRPD1A0842. IRB 97-2366B.

We appreciate the help from Dr. Yu-Chun Lin, Dr. Po-Han Wu, Ms. Wen-Shin Hung, and Mr. Kuan-Ying Lu for assistance in article preparation.

References

1. Amant F, Coosemans A, Debiec-Rychter M, Timmerman D, Vergote I. Clinical management of uterine sarcomas. Lancet Oncol 2009;10: 1188–1198.
2. Brooks SE, Zhan M, Cote T, Baquet CR. Surveillance, epidemiology, and end results analysis of 2677 cases of uterine sarcoma 1989–1999. Gynecol Oncol 2004;93:204–208.
3. Laughlin SK, Schroeder JC, Baird DD. New directions in the epidemiology of uterine fibroids. Semin Reprod Med 2010;28:204–217.
4. Guntupalli SR, Ramirez PT, Anderson ML, Milam MR, Bodurka DC, Malpica A. Uterine smooth muscle tumor of uncertain malignant potential: a retrospective analysis. Gynecol Oncol 2009;113:324–326.
5. Leibsohn S, d'Ablaing G, Mishell DR Jr, Schlaerth JB. Leiomyosarcoma in a series of hysterectomies performed for presumed uterine leiomyomas. Am J Obstet Gynecol 1990;162:968–974; discussion 974–966.
6. Metwally M, Cheong YC, Horne AW. Surgical treatment of fibroids for subfertility. Cochrane Database Syst Rev 2012;11:CD003857.
7. Gupta JK, Sinha AS, Lumsden MA, Hickey M. Uterine artery embolization for symptomatic uterine fibroids. Cochrane Database Syst Rev 2006:CD005073.

8. Kim HS, Baik JH, Pham LD, Jacobs MA. MR-guided high-intensity focused ultrasound treatment for symptomatic uterine leiomyomata: long-term outcomes. Acad Radiol 2011;18:970–976.
9. Wu TI, Yen TC, Lai CH. Clinical presentation and diagnosis of uterine sarcoma, including imaging. Best Pract Res Clin Obstet Gynecol 2011;25:681–689.
10. Sahdev A, Sohaib SA, Jacobs I, Shepherd JH, Oram DH, Reznek RH. MR imaging of uterine sarcomas. AJR Am J Roentgenol 2001;177: 1307–1311.
11. Tanaka YO, Nishida M, Tsunoda H, Okamoto Y, Yoshikawa H. Smooth muscle tumors of uncertain malignant potential and leiomyosarcomas of the uterus: MR findings. J Magn Reson Imaging 2004; 20:998–1007.
12. Yamashita Y, Torashima M, Takahashi M, et al. Hyperintense uterine leiomyoma at T2-weighted MR imaging: differentiation with dynamic enhanced MR imaging and clinical implications. Radiology 1993;189: 721–725.
13. Ueda H, Togashi K, Konishi I, et al. Unusual appearances of uterine leiomyomas: MR imaging findings and their histopathologic backgrounds. Radiographics 1999;19(Spec No):S131–145.
14. Cornfeld D, Israel G, Martel M, Weinreb J, Schwartz P, McCarthy S. MRI appearance of mesenchymal tumors of the uterus. Eur J Radiol 2010;74:241–249.
15. Tamai K, Koyama T, Saga T, et al. The utility of diffusion-weighted MR imaging for differentiating uterine sarcomas from benign leiomyomas. Eur Radiol 2008;18:723–730.
16. Namimoto T, Yamashita Y, Awai K, et al. Combined use of T2-weighted and diffusion-weighted 3-T MR imaging for differentiating uterine sarcomas from benign leiomyomas. Eur Radiol 2009;19:2756–2764.
17. Sato K, Yuasa N, Fujita M, Fukushima Y. Clinical application of diffusion-weighted imaging for preoperative differentiation between uterine leiomyoma and leiomyosarcoma. Am J Obstet Gynecol 2014; 210:368 e361–368.
18. Lin G, Ng KK, Chang CJ, et al. Myometrial invasion in endometrial cancer: diagnostic accuracy of diffusion-weighted 3.0-T MR imaging—initial experience. Radiology 2009;250:784–792.
19. Bell SW, Kempson RL, Hendrickson MR. Problematic uterine smooth muscle neoplasms. A clinicopathologic study of 213 cases. Am J Surg Pathol 1994;18:535–558.
20. Fleiss JL. Statistical methods for rates and proportions. New York: John Wiley & Sons; 1981.
21. Kido A, Togashi K, Koyama T, Yamaoka T, Fujiwara T, Fujii S. Diffusely enlarged uterus: evaluation with MR imaging. Radiographics 2003;23:1423–1439.
22. Hricak H, Tscholakoff D, Heinrichs L, et al. Uterine leiomyomas: correlation of MR, histopathologic findings, and symptoms. Radiology 1986;158:385–391.
23. Goto A, Takeuchi S, Sugimura K, Maruo T. Usefulness of Gd-DTPA contrast-enhanced dynamic MRI and serum determination of LDH and its isozymes in the differential diagnosis of leiomyosarcoma from degenerated leiomyoma of the uterus. Int J Gynecol Cancer 2002;12: 354–361.
24. Thomassin-Naggara I, Dechoux S, Bonneau C, et al. How to differentiate benign from malignant myometrial tumours using MR imaging. Eur Radiol 2013;23:2306–2314.
25. Shah SH, Jagannathan JP, Krajewski K, O'Regan KN, George S, Ramaiya NH. Uterine sarcomas: then and now. AJR Am J Roentgenol 2012;199:213–223.
26. Rha SE, Byun JY, Jung SE, et al. CT and MRI of uterine sarcomas and their mimickers. AJR Am J Roentgenol 2003;181:1369–1374.
27. Tirumani SH, Ojili V, Shanbhogue AK, Fasih N, Ryan JG, Reinhold C. Current concepts in the imaging of uterine sarcoma. Abdom Imaging 2013;38:397–411.
28. Wang Y, Alkasab TK, Narin O, et al. Incidence of nephrogenic systemic fibrosis after adoption of restrictive gadolinium-based contrast agent guidelines. Radiology 2011;260:105–111.